Mixed-Technology Quasi-Reflectionless Planar Bandpass Filters

Dakotah J. Simpson[1], Roberto Gómez-García[2], and Dimitra Psychogiou[1]
[1]Dept. of Electrical, Computer and Energy Engineering, University of Colorado at Boulder, USA
[2]Dept. of Signal Theory and Communications, University of Alcalá, Spain
Dakotah.Simpson@Colorado.edu

***Abstract* — This paper reports on the RF design of mixed-technology quasi-reflectionless planar bandpass filters (BPFs). They are based on a hybrid integration scheme in which microstrip resonators are effectively combined with lumped-element ones for size compactness. By loading the input and output ports of a first-order BPF with first-order bandstop-filter (BSF) sections that exhibit complementary transfer function with regard to the BPF one, a symmetric quasi-reflectionless behaviour can be obtained at both accesses of the overall filter. The first-order quasi-absorptive BPF cell can be extended to higher-rejection realizations by cascading in series multiple first-order stages and merging their interconnecting BSF sections. For experimental-validation purposes, two quasi-absorptive BPF prototypes (one- and two-stage schemes, respectively) centred at 2 GHz were designed, manufactured, and measured. They exhibit return-loss (RL) levels higher than 10 dB over fractional bandwidths (FBWs) of 117% and 111%, respectively.**

***Keywords* — absorptive filter, bandpass filter (BPF), lumped-element filter, microstrip filter, planar filter, reflectionless filter.**

I. Introduction

Due to the rise of new wireless communication systems that call for RF transceivers with low noise and interference-suppression capabilities, the need for bandpass filters (BPFs) with advanced RF functionality is increasing rapidly [1]. In particular, BPFs with as minimum as possible RF power reflection both in their passband and their stopband regions (i.e., reflectionless or absorptive) are crucial for the realization of RF front-ends with high signal-to-noise ratio (SNR). This is due to their potential of minimizing the overall RF signal-reflection levels that would otherwise give rise to instabilities. Note that typical BPF configurations are designed to reflect the non-transmitted signal energy back to the input, and therefore back into the transceiver chain, which can deteriorate the operation of adjacent actives stages and hence, of the whole system. As such, recent research efforts are focusing on reflectionless-type BPF implementation schemes.

Despite the advantages of reflectionless BPFs in terms of a more robust operation of their corresponding RF front-ends, recent developments have been mostly concentrating on reflectionless bandstop filter (BSF) configurations. Very few absorptive-type BPF architectures have been presented in the open technical literature up to date, and all of them with some limitations. A class of lumped-element reflectionless filters with theoretically-infinite input and output power matching at all frequencies was presented in [2]. However, the bandpass-type architecture requires a large number of lumped components for high-order designs and has high levels of in-band insertion loss (IL) (~4 dB). The architecture proposed in [3] is based on a parallel cascade of all-pass networks, but it makes use of directional couplers, leading to a considerable increase in its physical size and in-band IL levels (7 dB). In yet another configuration, lumped elements are used for the realization of lossy impedance matching networks that cancel out the reflected wave in the filter designs in [4]. However, they are limited to low frequencies and exhibit low selectivity. A class of fully-reflectionless adaptive BPF, BSF, and BPF-BSF cascades using complementary-duplexer channels was reported in [5]. However, despite being tunable, these non-symmetrical filter structures only exhibit the reflectionless behaviour at their input port.

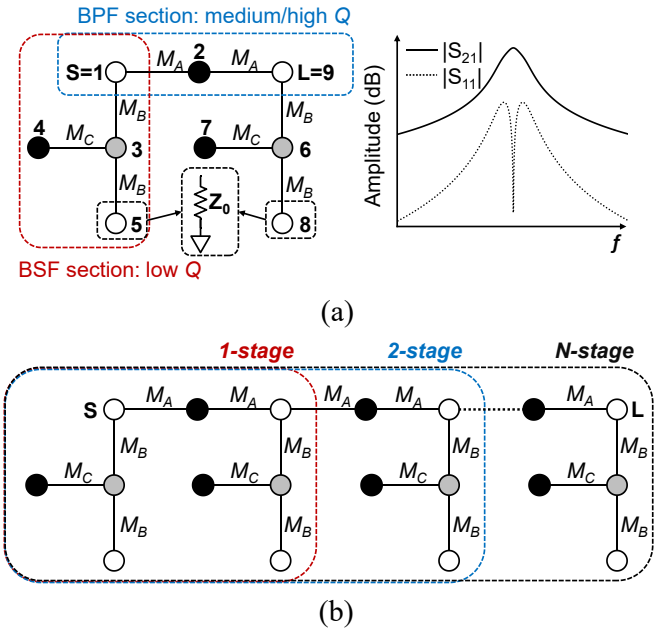

Fig. 1. Mixed-technology quasi-reflectionless BPF concept. (a) Coupling-matrix diagram of the first-order single-stage BPF and associated conceptual power transmission and reflection responses illustrating the quasi-reflectionless behaviour. White circles: source (S), load (L), and BSF-terminating resistors with resistance equal to the system impedance (Z_0), grey circles: non-resonating nodes, black circles: resonating nodes, and connecting lines: couplings. (b) Extension of the coupling-matrix diagram to a N-stage quasi-reflectionless BPF designs.

In this paper, the design of symmetrical quasi-absorptive BPFs is reported. The proposed filter concept allows for the realization of a symmetrical quasi-reflectionless behaviour. This is achieved by connecting first-order BSF sections at the input and output ports of its first-order BPF channel to absorb the reflected RF signals. In order to achieve size compactness, the proposed BPF configuration is implemented with a mixed-technology planar integration scheme that hybridizes microstrip-type resonators for the BPF channel and low-Q lumped-element resonators for the BSF section. In this manner, it is demonstrated that the quasi-reflectionless BPF concept is general even for resonators and impedance inverters with different frequency-dependence profile in its BPF and BSF branches.

The organization of this manuscript is as follows. In Section II, the theoretical background and main RF design principles of the proposed quasi-reflectionless BPF concept are presented through the analysis of its coupling-matrix diagram. The RF design of one- and two-stage BPF prototypes with a center frequency of 2 GHz and their experimental validation are reported in Section III. Lastly, a summary of the most relevant contributions of this work is given in Section IV.

II. Theoretical Background

The coupling-matrix diagram and conceptual transfer function of the proposed quasi-reflectionless BPF are illustrated in Fig. 1(a). The filter architecture consists of a medium- or high-Q BPF channel that is loaded at its input/output ports with resistively-terminated first-order BSF sections. The BPF is composed of a single resonator (resonating node 2) that is connected to the input/output ports through impedance inverters with coupling coefficients M_A. Each BSF section is made up of one resonating node (resonating nodes 4, 7) that is connected to a non-resonating node (nodes 3, 6) through an impedance inverter with a coupling coefficient M_C. The non-resonating node is also connected to the input (output) port of the BPF and a reference-impedance resistor Z_0, through impedance inverters that have coupling coefficients M_B. The quasi-reflectionless behaviour of the overall first-order filter is obtained when the BPF channel and the BSF sections exhibit complementary transfer functions. This is achieved when M_C is set equal to M_AM_B. In this case, the RF power that is not transmitted by the BPF is mostly absorbed by the resistors that are present in each BSF section. Furthermore, the coupling value M_A allows to control the passband bandwidth (BW) as shown in Fig. 2.

The first-order quasi-reflectionless BPF design can be used in higher-rejection multi-stage realizations by cascading in series multiple single-stage cells (like the one in Fig. 1(a)) and by merging their BSF sections at each junction. This is illustrated in Fig. 1(b). As it can be seen, a N-stage quasi-reflectionless architecture is composed of N resonators in its BPF section and N+1 resonators in its BSF sections that are interconnected through impedance inverters. Note that the coupling coefficients of the impedance inverters in the N-stage configuration are identical to the coupling coefficients of the single-stage design of Fig. 1(a).

To demonstrate the operational design principles of the presented quasi-reflectionless BPF concept, several ideally-synthesized responses are shown in Figs. 2-4. Specifically, Fig.

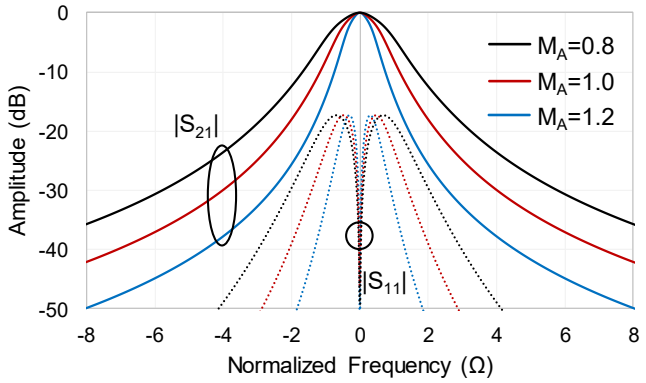

Fig. 2. Theoretically synthesized power transmission ($|S_{21}|=|S_{12}|$) and reflection ($|S_{11}|=|S_{22}|$) responses for a two-stage quasi-reflectionless BPF for alternative levels of M_A that result in passbands with different FBW. For all responses: $M_B=1$, $M_C=M_A$.

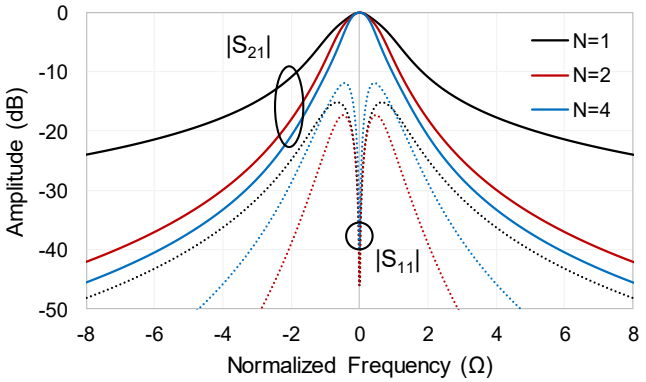

Fig. 3. Theoretically-synthesized power transmission ($|S_{21}|=|S_{12}|$) and reflection ($|S_{11}|=|S_{22}|$) responses for the quasi-reflectionless BPF in Fig. 1(b) for alternative number of stages N ($M_A=M_B=M_C=1$ in all responses).

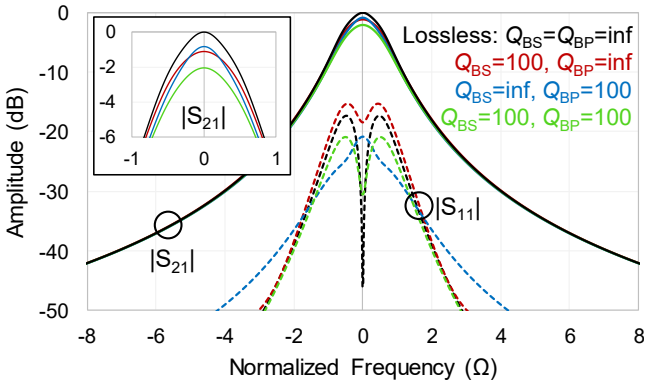

Fig. 4. Theoretically-synthesized power transmission ($|S_{21}|=|S_{12}|$) and reflection ($|S_{11}|=|S_{22}|$) responses for a two-stage quasi-reflectionless BPF (Q_{BS}: quality factor of the resonators in the BSF sections, Q_{BP}: quality factor of the resonators in the BPF channel, FBW=10%, and $M_A=M_B=M_C=1$ in all responses).

3 depicts the power transmission and reflection responses of one-, two-, and four-stage BPF designs. The single-stage design comes from the coupling matrix diagram provided in Fig. 1(a) whereas the two- and four-stage responses are synthesized using the coupling-matrix diagram in Fig. 1(b). As expected, by increasing the number of the cascaded sections, the out-of-band rejection levels of the filter increase. Furthermore, Fig. 2 corroborates the BW variation of a two-stage design by changing the coupling coefficient M_A. It should be noted that either one or both of the other coupling coefficients, M_B and M_C, need to be changed so as to retain the quasi-reflectionless behaviour by fulfilling the condition $M_C=M_AM_B$. Specifically, in the responses shown in Fig. 2, M_C is changed and M_B is left constant. In order to investigate the effect of the resonators' finite Q in the overall quasi-reflectionless BPF transfer function, the following power transmission and reflection responses have been synthesized for comparison purposes: i) lossless resonators, ii) lossy resonators in the BPF section (i.e., $Q_{BP}\neq\infty$), iii) lossy resonators in the BSF sections (i.e., $Q_{BS}\neq\infty$), and iv) lossy BPF and BSF resonators (i.e., Q_{BP},$Q_{BS}\neq\infty$). As it can be seen in Fig. 4, the passband IL loss is affected in this design by both the loss of the BPF and BSF resonators. However, despite the presence of IL in the BPF and BSF sections, the quasi-reflectionless behaviour is still attained.

III. Experimental Results

In order to experimentally validate the proposed quasi-reflectionless BPF concept, two prototypes –one- and two-stage architectures, respectively– with center frequency of 2 GHz were designed, manufactured, and measured. They were built on a Rogers RO4003C substrate with the following characteristics: relative permittivity ε_r=3.38, thickness H=1.52 mm, 1oz. copper cladding, and dielectric loss tangent tanδ_D=0.0021. Both designs were performed using the RF design principles in Section II and the software package Advanced Design System (ADS) from Keysight Technologies. For the filter implementation, a mixed-technology integration scheme has been followed. In particular, the BPF sections were realized through microstrip-type half-wavelength-at-2-GHz resonators and quarter-wavelength-at-2-GHz transmission line-based impedance inverters. The BSF sections were materialized by means of series-type lumped-element resonators and lumped-element impedance inverters for size compactness. In order to reduce the number of components, the parallel resonators were transformed to series through M_C and, as such, the impedance inverter M_C can be eliminated. Similarly, the impedance inverter M_B can be excluded by transforming the termination resistors Z_0 to M_B^2/Z_0.

The layout and a photograph of the manufactured single-stage quasi-absorptive BPF are shown in Fig. 5(a) and (b), respectively. Its RF performance was experimentally validated with a Keysight N5224A PNA in terms of S-parameters. A comparison of the RF-measured and EM-simulated power transmission and reflection responses and the group delay for this prototype are provided in Fig. 6, successfully validating the proposed quasi-reflectionless BPF concept. Its main measured

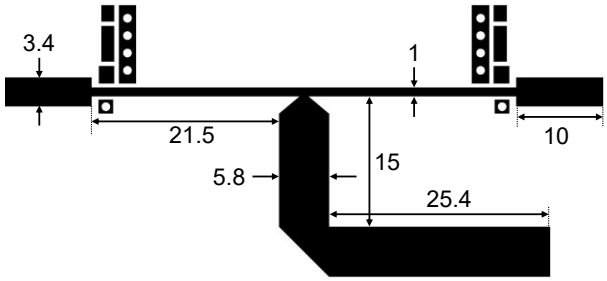

(a)

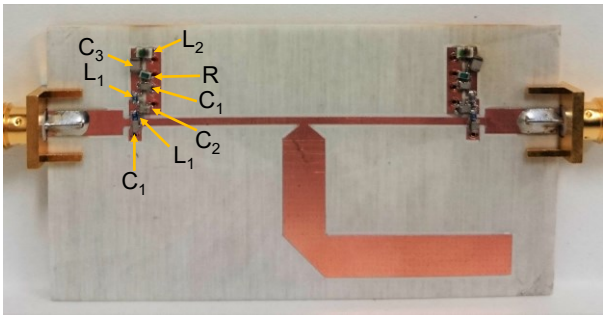

(b)

Fig. 5. (a) Layout of the single-stage quasi-reflectionless BPF (dimensions in mm). (b) Photograph of the manufactured prototype. Overall dimensions: 68.8x37.3 mm^2. R=46 Ω. All inductors are from Coilcraft: L_1=2.4 nH (0402HP-2N4) and L_2=10 nH (0805HT-10N). All capacitors are from Johanson Technology: C_1=0.3 pF (251R14S0R3BV4S), C_2=1.0 pF (251R14S1R0BV4S), and C_3=0.3 pF (251R15S0R3BV4S).

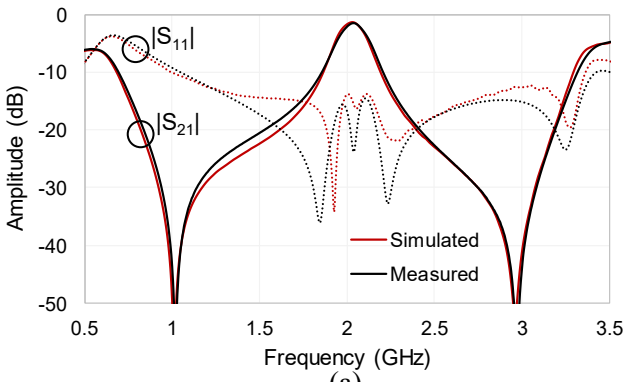

(a)

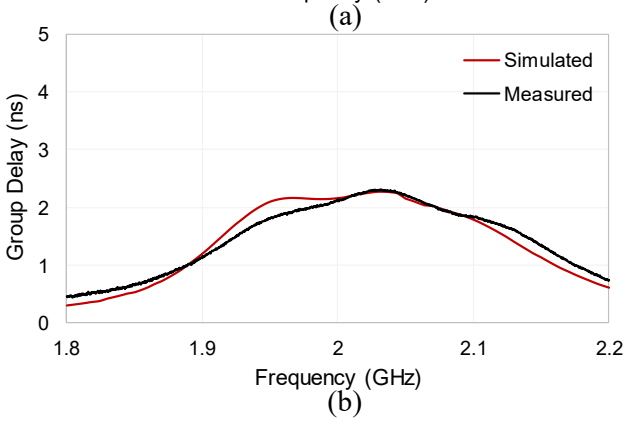

(b)

Fig. 6. RF-measured and EM-simulated responses of the single-stage quasi-reflectionless BPF in Fig. 5. (a) Power transmission ($|S_{21}|$) and reflection ($|S_{11}|$) responses. (b) Detail of the group delay.

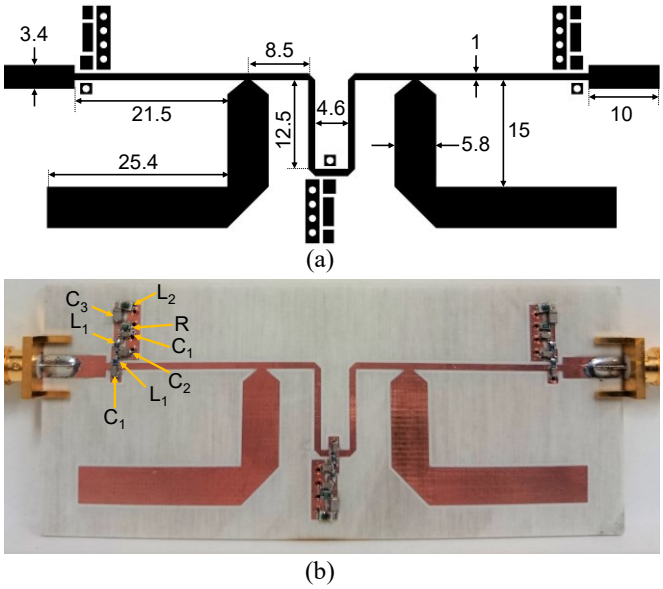

Fig. 7. (a) Layout of the two-stage quasi-reflectionless BPF (dimensions in mm). (b) Photograph of the manufactured prototype. Overall dimensions: 92.4x39.5 mm^2. R=46 Ω. All inductors are from Coilcraft: L_1=2.4 nH (0402HP-2N4) and L_2=10 nH (0805HT-10N). All capacitors are from Johanson Technology: C_1=0.3 pF (251R14S0R3BV4S), C_2=1.0 pF (251R14S1R0BV4S), and C_3=0.3 pF (251R15S0R3BV4S).

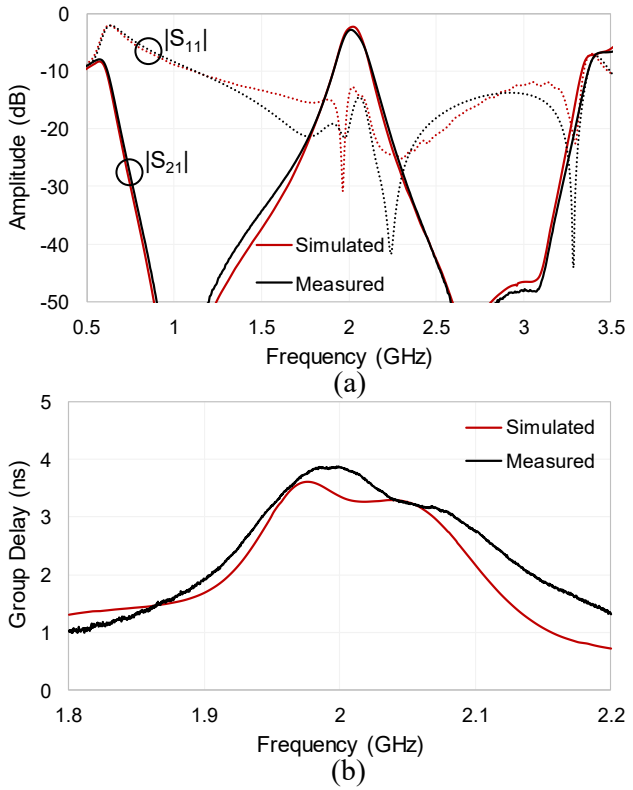

Fig. 8. RF-measured and EM-simulated responses of the two-stage quasi-absorptive BPF in Fig. 7. (a) Power transmission ($|S_{21}|$) and reflection ($|S_{11}|$) responses. (b) Detail of the group delay.

RF performance metrics can be summarized as follows: center frequency of 2.04 GHz, BW of 184 MHz (i.e., of 9%), minimum in-band IL of 1.49 dB, group delay less than 3.1 ns, and return-loss (RL) levels greater than 14.5 dB throughout the passband and larger than 10 dB in the range 1.04-3.43 GHz (i.e., 3.3:1 ratio). This corresponds to a quasi-reflectionless fractional bandwidth (FBW) of 117%.

The second prototype that was manufactured for validation purposes is a two-stage quasi-absorptive BPF based on the extension of the design of the single-stage prototype (i.e., the same component values were used). Its layout and a photograph are presented in Fig. 7(a) and (b), respectively. The RF-measured and EM-simulated power transmission and reflection responses and the group delay of this circuit are compared in Fig. 8, showing again a fairly close agreement. Its main measured RF performance characteristics are as follows: center frequency of 2.01 GHz, BW of 140 MHz (i.e., of 7%), minimum in-band IL of 2.78 dB, group delay less than 4.3 ns, and RL levels greater than 14.4 dB throughout the passband and over 10 dB in the range 1.13-3.37 GHz (i.e., 3:1 ratio). This corresponds to a quasi-reflectionless FBW of 111%.

IV. Conclusion

A new class of planar BPFs with symmetric quasi-reflectionless characteristics has been presented. They are based on first-order BPF sections that are loaded at their input and output ports with resistively-terminated first-order BSF branches that exhibit complementary transfer functions. The quasi-reflectionless behaviour is obtained by absorbing the RF-signal energy from the stopband regions of the BPF section. For size compactness and in order to evaluate the practical viability of the proposed quasi-reflectionless BPF concept, a mixed-technology integration scheme was adopted in which the BPF sections were materialized with microstrip elements and the BSF ones with lumped elements. Two BPF prototypes, namely a one- and a two-stage circuit, were designed at 2 GHz, manufactured, and measured.

Acknowledgment

This work has been supported in part by the National Science Foundation, award number 1731956, the Dean's Graduate Assistantship (DGA) of the University of Colorado at Boulder, and by the Spanish Ministry of Economy and Competitiveness under Project TEC2017-82398-R. The authors would like to thank Keysight for providing access to the software package ADS.

References

[1] W. J. Chappell, E. J. Naglich, C. Maxey, and A. C. Guyette, "Putting the radio in "Software-defined radio": Hardware developments for adaptable RF systems," *Proc. of IEEE*, vol. 102, no. 3, pp. 307-320, March 2014.

[2] M. A. Morgan and T. A. Boyd, "Theoretical and experimental study of a new class of reflectionless filter," *IEEE Trans. Microw. Theory Techn.*, vol. 59, no. 5, pp. 1214–1221, May 2011.

[3] A. C. Guyette, I. C. Hunter, and R. D. Pollard, "Design of absorptive microwave filters using allpass networks in a parallel-cascade configuration," in *Proc. IEEE MTT-S Int. Microw. Symp.*, Boston, MA, USA, 2009, pp. 733–736.

[4] T.-H. Lee, B. Lee, and J. Lee, "First-order reflectionless lumped-element lowpass filter (LPF) and bandpass filter (BPF) design," in *Proc. IEEE MTT-S Int. Microw. Symp.*, San Francisco, CA, 2016, pp. 1–4.

[5] D. Psychogiou and R. Gómez-García, "Reflectionless adaptive RF filters: bandpass, bandstop, and cascade designs," in *IEEE Trans. Microw. Theory Techn.*, vol. 65, no. 11, pp. 4593–4605, Nov. 2017.